

# Characterization of Receiver Demodulation for Correcting Off-axis MR Imaging Degradation

Y. Jung<sup>1</sup>, Y. Jashnani<sup>2</sup>, R. Kijowski<sup>3</sup>, W. F. Block<sup>2,4</sup>

<sup>1</sup>Electrical and Computer Engineering, University of Wisconsin-Madison, Madison, WI, United States, <sup>2</sup>Biomedical Engineering, University of Wisconsin-Madison, Madison, WI, United States, <sup>3</sup>Radiology, University of Wisconsin-Madison, Madison, WI, United States, <sup>4</sup>Medical Physics, University of Wisconsin-Madison, Madison, WI, United States

## INTRODUCTION

The consistency of imaging with non-Cartesian sequences across a large number of scanners is highly variable. Improper alignment of the gradient coil and the real-time frequency demodulation reference signal, necessary in off-axis imaging, may be one source of this variability. As the system delay parameter used to guarantee alignment varies with imaging bandwidth and between scanners, many non-Cartesian imaging methods require trial and error tuning for off-axis imaging. In addition, the minimum quantized intervals over which the reference signal can be shifted are too large for the rapid imaging possible today. We present an automatic per-patient-based method to precisely measure the timing error in the frequency demodulation reference signal in less than 0.5 s. We also demonstrate significant image quality improvement by removing phase errors due to the improper timing.

## MATERIALS AND METHODS

The timing error is measured by examining the difference in the phase of signals from two successive MR excitations. In the first, a thin offset slice is excited, rephased, and encoded by a bipolar gradient waveform on the same axis, as illustrated in Fig. 1. This waveform also serves as the receiver's real-time frequency demodulation reference signal,  $\Delta f(t)$ , which tracks the phase of the excited slice. In the second excitation, the process is repeated with  $\Delta f(t)$  set to zero. By subtracting the phase measured in each excitation, phase errors due to off-resonance, concomitant gradients, eddy currents, and mistuned delays between the gradient and data acquisition hardware are removed. Remaining phase differences are due to the timing error in the demodulation hardware and a bias due to miscalibration in the slice select gradient amplitude.

The phase difference due to an improperly delayed frequency reference signal has the same shape as  $\Delta f(t)$ , as shown in Fig. 2a. If the exact slice location is not excited due to a slight miscalibration in gradient strength, a bias (Fig. 2b) will distort the phase difference and appear as in Fig. 2c. Taking the difference between average values of phase error from the flat-tops of the bipolar gradient can remove the bias and provides the maximum phase error ( $E_{\Phi_{MAX}}$ ). The timing error  $\tau$  in the reference signal can be calculated as  $\tau = E_{\Phi_{MAX}} / (2\pi \gamma G_{MAX} d)$ , where  $G_{MAX}$  is the peak gradient strength and  $d$  is the offset distance of the excited slice.

The timing error was measured on four Signa EXCITE HD scanners (GE Healthcare, Milwaukee, WI). A subject's knee was imaged in its natural position, 6 cm laterally off-axis, using a dual half-echo VIPR-SSFP [1] sequence, a 18 cm FOV, and  $\pm 125$  kHz BW. Using knowledge of the timing error, we retrospectively corrected demodulation phase errors during the VIPR reconstruction. Furthermore, to demonstrate improvements in another non-Cartesian sequence, we imaged a phantom positioned 5 cm laterally off-axis with a commercially available spiral sequence after rounding the measured delay to the nearest quantized system delay achievable.

## RESULTS AND DISCUSSION

The measurement of  $E_{\Phi_{MAX}}$  was signal averaged by repeating this algorithm over a 0.5 s to generate a precision of 0.1  $\mu$ s in  $\tau$ . The timing delays of four scanners were measured to be 4.2 to 7.5  $\mu$ s above the manufacturer suggested delay. Significant degradation in the VIPR knee image, Fig. 3a, is retrospectively corrected in Fig. 3b. Although the manufacturer allows the reference signal to be shifted at quantized 2  $\mu$ s intervals, even a 1  $\mu$ s error will produce a significant 60° phase error between the dual echoes in this sequence. The spiral image, prior to adjusting the delay, shows blurring along edges perpendicular to the offset direction in Fig. 3c. Adjusting the delay to the nearest quantized interval removes this blurring (Fig. 3d).

The relationship between timing error and receiver bandwidth was examined and was found similar to the results of Speier et al. [2], its linear relationship can be expressed as  $\tau = -0.5 * t_{\text{sampling}} + C$ , where  $t_{\text{sampling}}$  is the data sampling interval for a given bandwidth and C is a scanner-dependent timing error.

If unlimited receiver bandwidth were possible, off-axis demodulation could simply be performed during reconstruction and this hardware delay could be ignored. Limits in receiver bandwidth and the extra k-space storage requirements, especially with the growing number of MR coils, make real-time demodulation necessary.

## CONCLUSIONS

A rapid method of precisely quantifying the real-time frequency demodulation system delay without operator intervention has been presented. Off-axis image quality is significantly improved when compensation for demodulation phase errors due to the delay is performed. We have demonstrated the algorithm on radial and spiral imaging, but the benefits would apply to other non-Cartesian imaging methods. The method may allow more consistent performance of non-Cartesian sequences over a large installed base of scanners.

**ACKNOWLEDGEMENTS** The research was supported by NIH 8 R01 EB002075-07 and GE Healthcare.

**REFERENCES** 1. Lu AM, et al., MRM, 53, 692, 2005. 2. Speier P, et al., Proc. 13th ISMRM, 2295, 2005.

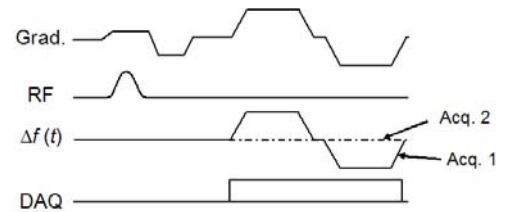


FIG. 1. Pulse sequence block for measuring timing error.

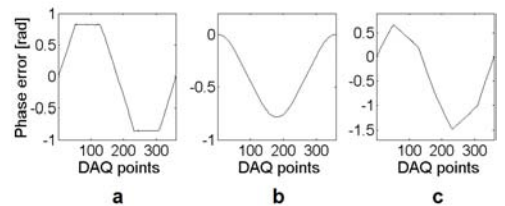


FIG. 2. Phase error from a timing error (a) and a bias (b) comprise the measured phase difference in (c).

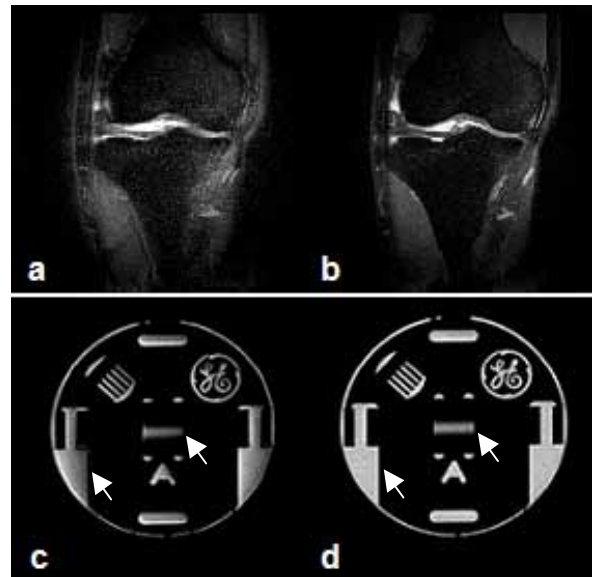


FIG. 3. Result of correction using the measured timing error ( $\tau$ ) in VIPR (top row) and spiral (bottom row) sequences. Image degradation before correction (a, c) was dramatically improved after correction (b, d)